
This document presents a review of available literature related to the 1979 Cadoux surface rupturing earthquake. It includes newly digitised data related to the rupture and new interpretations of controls on fault rupture. It is intended to supplement a manuscript reviewing all Australian surface rupturing earthquakes, submitted to Geosciences in August 2019. It may be repackaged for submission to a peer-reviewed journal at a later date and we consider it to be a draft pre-print.

Please contact any of the authors on the content presented herein; we welcome constructive feedback.

Review paper: The 2nd June 1979 M_w 6.1 Cadoux surface rupturing earthquake, Australia

Tamarah King

School of Earth Sciences, The University of Melbourne, Victoria 3010, Australia
tamarah.king@unimelb.edu.au
<https://orcid.org/0000-0002-9654-2917>

Mark Quigley

School of Earth Sciences, The University of Melbourne, Victoria 3010, Australia
Mark.quigley@unimelb.edu.au
<https://orcid.org/0000-0002-4430-4212>

Dan Clark

Geoscience Australia, Canberra 2601, Australia
Dan.Clark@ga.gov.au
<https://orcid.org/0000-0001-5387-4404>

Abstract

The 2nd June 1979 moment magnitude (M_w) 6.1 Cadoux earthquake caused a complex, multi-fault surface rupture consisting of six mapped scarps: (from south to north) the 8 km long west dipping Robb scarp, 3 km long south dipping Cumming scarp, the Lone Tree, Carter and Tank scarps (which together define an east-dipping arcuate rupture) and the 2.5 km long southwest-dipping Kalajzic scarp. Surface ruptures are classified as six intersecting faults using kinematic and orientation criteria, with a total simplified surface rupture length of 20.6 km (47% greater than lengths previously published in earthquake scaling relationship analyses). These faults align with structural trends in basement geology as mapped from surface outcrops and geophysical maps. No prior attempts have been made to reconcile seismological data with the geometrically complex surface rupture in order to investigate rupture initiation and propagation. We speculate that this earthquake ruptured unilaterally (from south to north) towards an area of increased structural complexity, within which the rupture eventually terminated. Aftershock locations have large epistemic uncertainties and do not enable accurate constructions of sub-surface fault geometry. Descriptions of shallow trenches across the Carter and Tank scarps suggest no prior rupture along at least some of the Calingiri scarps between the formation of basement structures (Archean – Proterozoic) and Tertiary – Quaternary surface sedimentation. The Cadoux earthquake is one of the most structurally complex earthquakes globally for this moderate (i.e., M_w ≤ 6.1) magnitude.

1. Geology

1.1 Regional / background

The 1979 M_w 6.1 Cadoux earthquake is one of a series of historical surface rupturing earthquakes (1968 Meckering, 1970 Calingiri, 1979 Cadoux, 2008 Katanning, and 2018 Lake Muir) (Dawson et al., 2008; Gordon and Lewis, 1980; Lewis et al., 1981) hosted within the South-West Seismic Zone (SWSZ) in southern Western Australia (Doyle, 1971). The SWSZ resides predominately within the Yilgarn Craton (*Figure 1*), an assemblage of predominately Archean granitoid-greenstone rocks (Wilde et al., 1996). The SWSZ extends roughly NW-SE within a region of the Yilgarn Craton consisting of poly-deformed and metamorphosed crystalline basement (*Figure 1*). The SWSZ extends across three tectono-stratigraphic terranes; the Boddington Terrane, Lake Grace Terrane and Murchison Terrane (Dentith and Featherstone, 2003; Wilde et al., 1996). Due in part to few basement

outcrops, the boundaries between terranes are poorly constrained. Gravity data show that the boundary between the Boddington and Lake Grace Terranes is a major east-dipping geological structure (Clark et al., 2008; Dentith and Featherstone, 2003), interpreted as a large thrust zone based on dating and metamorphic facies analysis across the two terranes (Wilde et al., 1996). Historic seismicity generally aligns with this structure, and occurs on the eastern side of it (Dentith and Featherstone, 2003).

The Cadoux earthquake occurred at the northern extent of SWSZ near the boundary of the Murchison Terrane with the Southern Cross Province (Clark et al., 2008; Dentith and Featherstone, 2003). The rupture seems to have occurred within the Southern Cross Province, though the boundary locations are poorly defined (Figure 1).

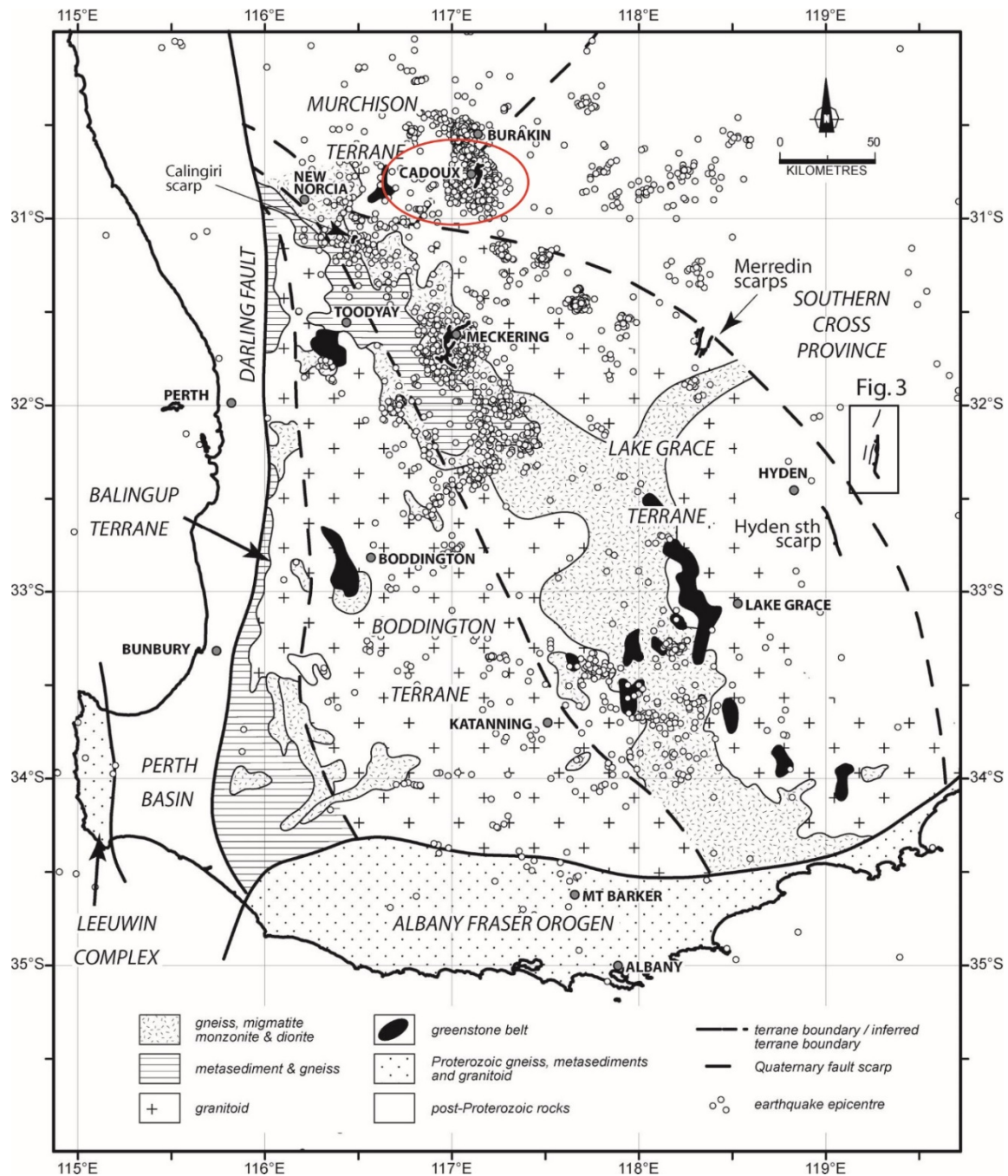


Figure 1: Regional geology surrounding the Cadoux earthquake (red circle) and SWSZ seismicity up to 2008: Figure 2 from Clark et al. (2008)

1.2 Local units / bedrock

Bedrock in the Cadoux area is mapped as metamorphosed granites (Blight et al., 1983; Lewis et al., 1981). Many of the outcrops have strike and dip measurements on the 1: 250 000 geological map (Blight et al., 1983) (*Figure 3*), described as “igneous foliations” with a predominately eastward dip and strike N-S or NW-SE, subparallel to different strands of the complicated surface rupture. Xenoliths of gneiss and amphibolite are reported within granites west of the surface rupture, in the direction of the Murchison Terrane boundary. Dolerite dykes are mapped across the area with two distinct orientations to the west, and to the northwest. Granite outcrops have widely spaced subvertical jointing orientated variably with an average strike of 060° ($040 - 070^{\circ}$), or 315° ($300 - 340^{\circ}$) (Lewis et al., 1981). Earthquake fracturing was observed to have caused dilation of these joints up to 2mm (Gordon and Lewis, 1980), though this may relate to shaking rather than primary fault movement. The northern extent of rupture interacts with surface bedrock outcrops, with one section of scarp rupturing through granite, and another following a line of granite outcrops on the hanging-wall and footwall. Many of the mapped foliation and intrusion orientations are evident on the total magnetic intensity map, which shows how different segments of surface rupture align to these various structural orientations (*Figure 2*). The overall strike of surface rupture is also subparallel to a gravity anomaly, with a slight gravitational high on the western side of rupture (*Figure 2*).

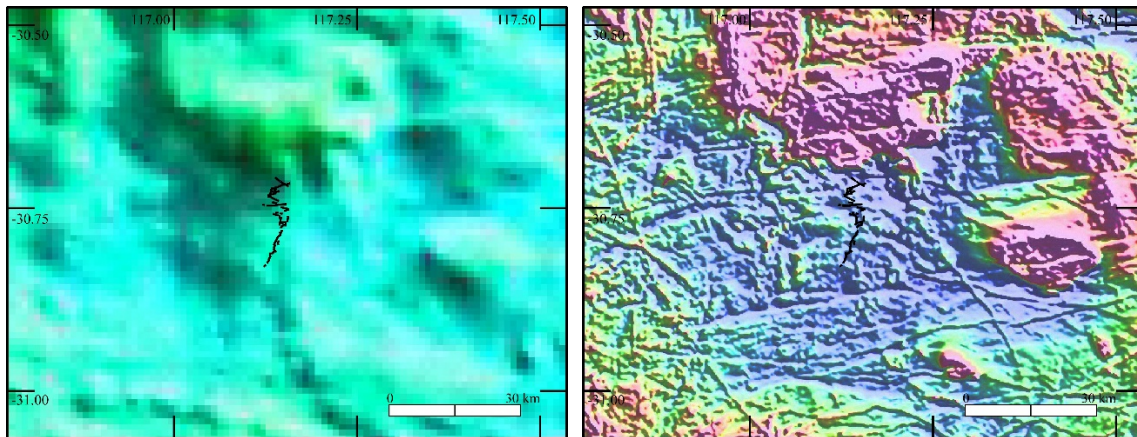
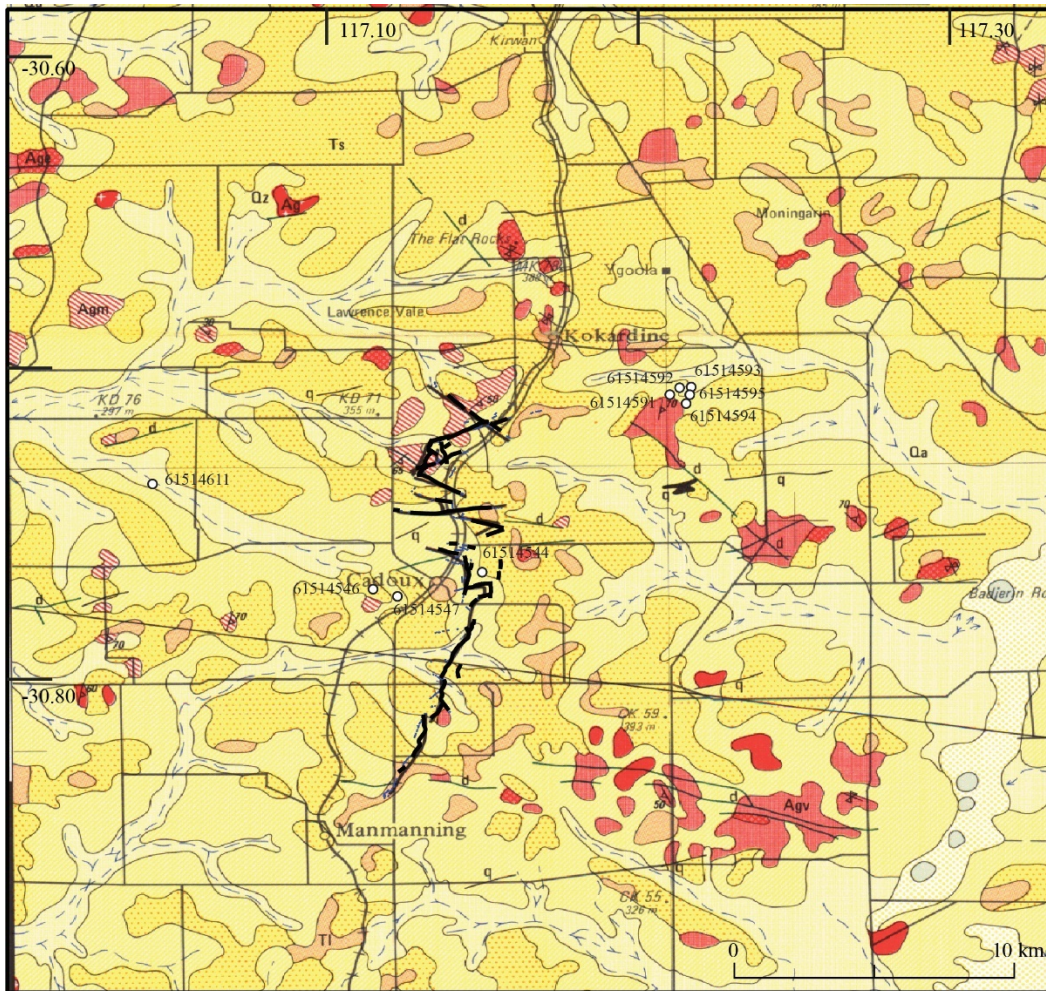


Figure 2: Cadoux scarp (black lines) relative to magnetic intensity and bouguer gravity anomaly maps. National bouguer gravity anomaly map: <http://pid.geoscience.gov.au/dataset/ga/101104>; National total magnetic intensity map: <http://pid.geoscience.gov.au/dataset/ga/89596>

1.3 Surficial deposits

Lewis et al. (1981) describe surface deposits in the area as alluvium-filled valley floors, laterite with overlying sandplain, and rock exposures with colluvium. The laterite and sand unit are described as 5 – 20 m thick, while colluvium is up to 30 m thick overlying either the latter unit, or bedrock. More detail is provided on the 1:250 000 geological map of the area (Blight et al., 1983) (*Figure 3*) reproduced in Plate 1 of Lewis et al. (1981).



| | | |
|------------|-----|--|
| Quaternary | Qa | Alluvium - clay, silt, sand and gravel, valley fill |
| | Qz | Mixed sheetwash deposit, colluvium and alluvium - red-brown sandy and clayey loam on valley slopes |
| Tertiary | Ts | Sand, yellow-white - commonly contains limonite nodules. Remnant of Tertiary sandplain |
| | Tl | Laterite and silcrete - grades upward into Ts and downward into weathered bedrock |
| Archaean | Ag | Granitoid, unassigned |
| | Agv | Variable textured adamellite: medium and coarse-grained, commonly seriate, microcline phenocrysts, biotite clots and abundant fluorite |
| | Agm | Mixed granite rocks not separable on map scale; includes pervasive pegmatite |
| | Age | Biotite adamellite and granite: medium and fine-grained, equigranular, allotriomorphic |

| | |
|---|------------------------|
| ◆ | Foliation, metamorphic |
| ◇ | Foliation, igneous |
| ▬ | Dolerite dykes |
| ▬ | Quartz veins |

Bencubbin 1:250 000 geological map
Geological Survey of Western Australia
1979
Copyright to GSWA / WA Gov.
Legend reproduced and condensed
for legibility from original

| Available lithological logs from groundwater bore-hole data - WIN database | | | |
|--|------------------------------|----------------------------|--|
| 61514546 | 61514547 | 61514544 | 61514592 |
| (m) Desc. | (m) Desc. | (m) Desc. | "bottomed on granite" (drill depth 4.2) |
| 0.0-1.4 hard rock | 0-0.9 clay | 0.0 - 0.3 sand | 61514591 |
| 1.4-4.1 sandstone | 0.9-6.1 hard rock | 0.3-1.2 clay | "bottomed on granite" (drill depth 5.1m) |
| 4.1-8.4 decomposed granite | 6.1-28.3 sandstone | 1.2-3.0 conglomerate | 61514594 |
| 8.4-9.1 hard rock | 28.3-34.4 decomposed granite | 3.0-19 rock | "bottomed on granite" (drill depth 19.5m) |
| 9.1-12.3 granite | | 19-19.6 decomposed granite | 61514593 |
| | | 19.6-20.5 granite | "cement, kaolin, decomposed granite" (drill depth 28m) |
| 61514611 | | | 61514595 |
| "sand, cement, sandstone, conglomerate" (drill depth 28.3m) | | | "ironstone, decomposed ironstone" (drill depth 25.9m) |

Water INformation (WIN) database - discrete sample data. [accessed: 17/07/2019].
Department of Water and Environmental Regulation, Water Information section, Perth Western Australia.

Figure 3: Crop of Bencubbin 1:250 000 geological map sheet (Blight et al., 1983), the only known geological map around the Cadoux rupture, and available ground-water bore-hole lithological logs from the area. Full map and legend available from: <http://www.dmp.wa.gov.au/Geological->

Survey/GSWA-publications-and-maps-1399.aspx. Full groundwater data available from: <http://wir.water.wa.gov.au/Pages/Water-Information-Reporting.aspx>. Lewis et al. (1981) reproduce this map in greyscale in Plate 1 of that report.

2. Seismology

2.1 Epicentre and magnitude estimates

Table 1 lists published epicentre coordinates, hypocentral depths and magnitude values for the Cadoux earthquake. The epicentral location in the current Geoscience Australia (GA) online catalogue is derived from Denham et al. (1987) who recalculated parameters from Australian stations based on an updated velocity model. This location is 4 km SW of the original USGS location, and 3 km east of the originally reported location from the Mundaring Geophysical Observatory (Gregson and Paull, 1979; Lewis et al., 1981). Denham et al. (1987) report epicentral uncertainties of ± 2 km which are relatively low considering the instrumental density available at the time of the event (Leonard, 2008). The GA NSHA18 catalogue (Allen et al., 2018) has a location 8.3 km west of the GA online catalogue, making it the only epicentre on the western side of the scarps (*Figure 4*). We favour a southern location for the epicentre, relative to the entire observed length of the surface rupture zone, given the increased density of proposed and more precisely constrained (due to increased seismic analysis including relocations) epicentral locations placed in this area.

This paper prefers the magnitude (M_w) of the recently published NSHA18 catalogue (Allen et al., 2018) as they conduct a thorough and consistent reanalysis of Australian magnitude values, particularly to address inconsistencies in the determination of historic magnitude values. Prior to this reanalysis, the magnitude of the Cadoux earthquake was reported as 5.9 – 6.2 using various local magnitude formula (M_L), and up to 6.4 surface wave magnitude (M_s).

Table 1 : Published epicentre locations, depths and magnitudes

| Reference | Agency | Latitude | \pm (km) | Longitude | \pm (km) | Depth | \pm (km) | M1 | | M2 | | M3 | |
|---------------------------|--------|----------|------------|-----------|------------|-------|------------|-----|----|-----|----|-----|----|
| (Denham et al., 1987) | | -30.83 | | 117.18 | | 6 | | 5.9 | ML | 6 | Ms | 6.2 | ML |
| GA_online | GA | -30.827 | | 117.179 | | 3 | | 6.1 | Mw | 6.2 | ML | 6 | Mb |
| (Gregson and Paull, 1979) | GA | -30.83 | | 117.15 | | 15 | | 6.2 | ML | | | | |
| (Denham et al., 1987) | USGS | -30.73 | | 117.2 | | 6 | | | | | | | |
| (Lewis et al., 1981) | | -30.83 | 2 | 117.15 | 2 | 15 | 5 | 6.2 | ML | 6.4 | Ms | 6.3 | Mb |
| (Allen et al., 2018) | | -30.821 | | 117.104 | | 3 | | 6.1 | Mw | | | | |
| (Denham et al., 1987) | USGS | -30.8 | | 117.2 | | | | | | | | | |

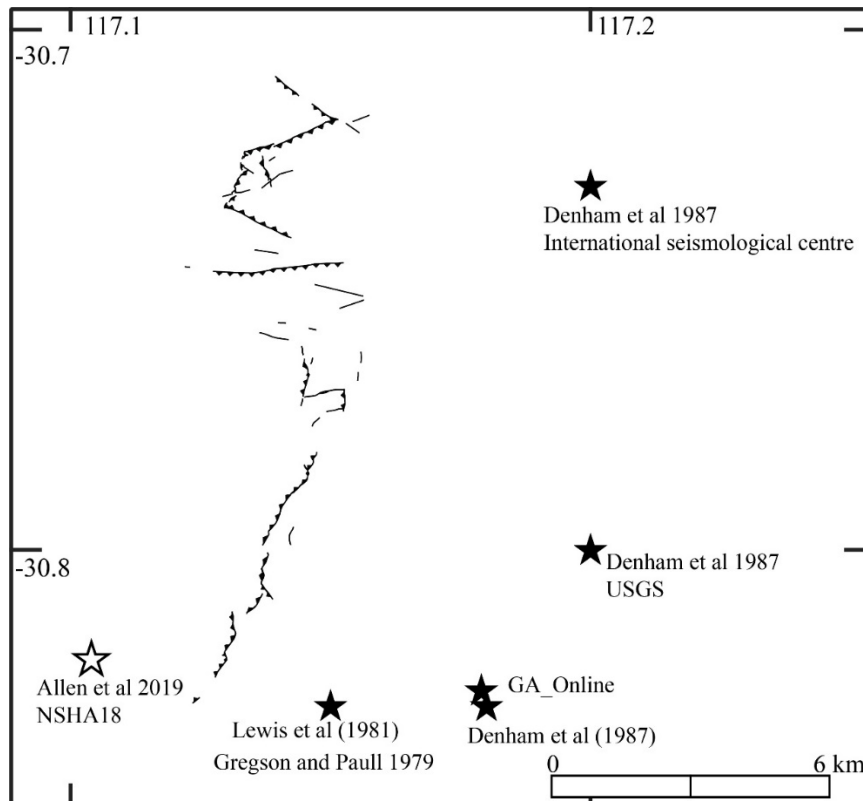


Figure 4: Published epicentre locations around the surface rupture. NSHA18 open star shows an unknown derivation of epicentre location within that catalogue.

2.2 Focal mechanisms

Three published focal mechanisms exist for the Cadoux mainshock (Denham et al., 1987; Fredrich et al., 1988, CMT Harvard catalogue) and one unpublished mechanism is discussed in Lewis et al. (1981) attributed to “Everingham and Smith” (Figure 5). Denham et al. (1987) and Fredrich et al. (1988) use teleseismic P- and SH- waves in their solution. There are no descriptions in Lewis et al. (1981) describing the methods used by Everingham and Smith to derive their focal mechanism. The published mechanisms show predominately reverse movement on a roughly N-S orientated fault. The Fredrich et al. (1988) solution shows pure thrust, while the Denham et al. (1987) and CMT solutions show opposing minor lateral components. Lewis et al. (1981) prefer the southwest dipping solution with a sinistral sense of movement, though they note that the N-S dextral thrust solution fits the strike of observed rupture better.

Choosing a preferred plane and deriving a dip from seismological data is highly uncertain as segments of surface rupture show both west over east, and east over west senses of movement (Section 3.2). Denham et al. (1987) prefer an overall east over west movement which matches their steeper 67° east dipping plane while Fredrich et al. (1988) show results for the shallower $34^\circ (\pm 7)$ west dipping plane. Lewis et al. (1981) prefer a south-west dipping mechanism solution with a 64° dip. Section 3.5 describes how surface rupture geometry, surface displacement measurements, and aftershock distribution relate to seismologically derived dip measurements.

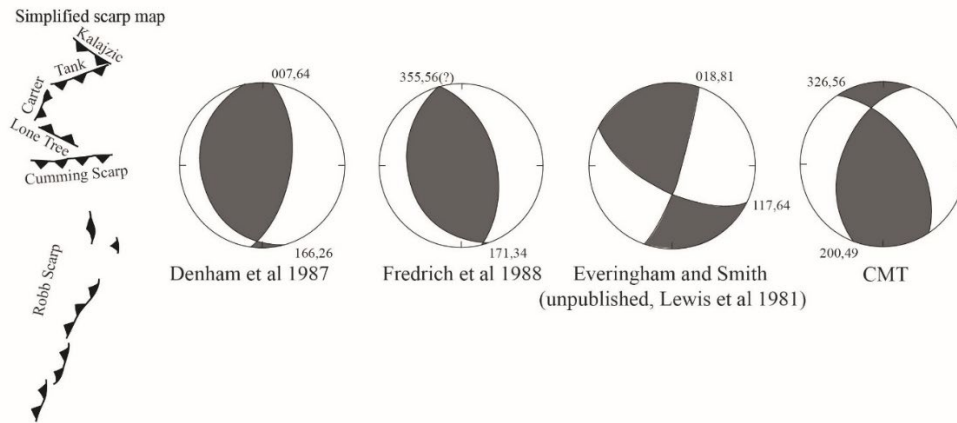


Figure 5: Published focal mechanism and simplified scarp map.

2.3 Depth

Fredrich et al. (1988) suggest a centroid depth of 4 – 6 km based on best-fit inversions of synthetic and observed long period data from nearby seismometers. Denham et al. (1987) present a hypocentral depth of 6 km in their relocation using an updated velocity model. The original hypocentre depth reported by the Mundaring Observatory is 15 ± 5 km (Gregson and Paull, 1979; Lewis et al., 1981) which is too deep to produce a surface rupture.

2.1 Foreshock / aftershocks

One M_L 3.6 was recorded in late 1978 (seven months prior), four earthquakes of M_L 3.1 - 3.9 in March 1979 (three months prior), three small earthquakes M_L 2.0 - 3.9 in April-May 1979 (two-one month), and 12 hours prior to the mainshock a M_L 5.2 was recorded followed by five M_L 3.0 - 3.8 earthquakes (Gregson and Paull, 1979; Lewis et al., 1981). Foreshocks are mapped south of the town in the vicinity of the mainshock with uncertainties of ~ 10 km estimated by Denham et al. (1987). Lewis et al. (1981) suggest that increased foreshock activity in the months preceding the mainshock could have been noted as anomalous. However, Gregson and Paull (1979) note that no other SWSZ earthquakes had had similar sized foreshocks. The location of foreshock activity is relatively scattered across the east and west sides of the 1979 surface rupture.

The largest aftershocks of M_L 5.3, 5.5, and 4.3 occurred one, five and eight days following the mainshock. Within the first twelve days, the Mundaring Geophysical Observatory recorded 123 aftershocks $M_L > 2.4$. A dense array of temporary seismometers operated during Oct-Nov 1983 (four years following the mainshock) allowed high accuracy location of ~ 35 aftershocks $M_L < 2.4$ (Dent, 1988). Aftershocks in the months following the mainshock are mapped on the eastern side of the rupture (Lewis et al., 1981), though these locations have higher uncertainties. Relocated aftershock locations from national data (Denham et al., 1987) shows seismicity from 1980 – 1983 increasingly around the northern and southern extents of surface rupture. Locations from a dense aftershock array (Dent, 1988; Dent and Gregson, 1986) show increased seismicity on the western side of the rupture in 1983. These later studies show migrating zones of high seismicity in the years following the Cadoux mainshock, though they also highlight high uncertainties in the original aftershock locations.

3. Surface Rupture

3.1 Authors / map quality

The Cadoux surface rupture occurred through pastoral properties a 220 km drive from Perth and is therefore accessible by road. Surface rupture mapping and investigations were undertaken in the six weeks following the earthquake by Geological Survey of Western Australia employees (Gregson and

Paull, 1979; Lewis et al., 1981). The only published map of the surface rupture is in Lewis et al. (1981) at a 1:25,000 scale. The rupture trace from this map is reproduced in the GA Neotectonics Features database (Clark, 2012). Lewis et al. (1981) note that observable surficial rupture had been destroyed by farming, however some sections of the rupture are still visible across ploughed fields in Google and Bing satellite imagery (e.g. -30.79, 117.14 to -30.78, 117.144).

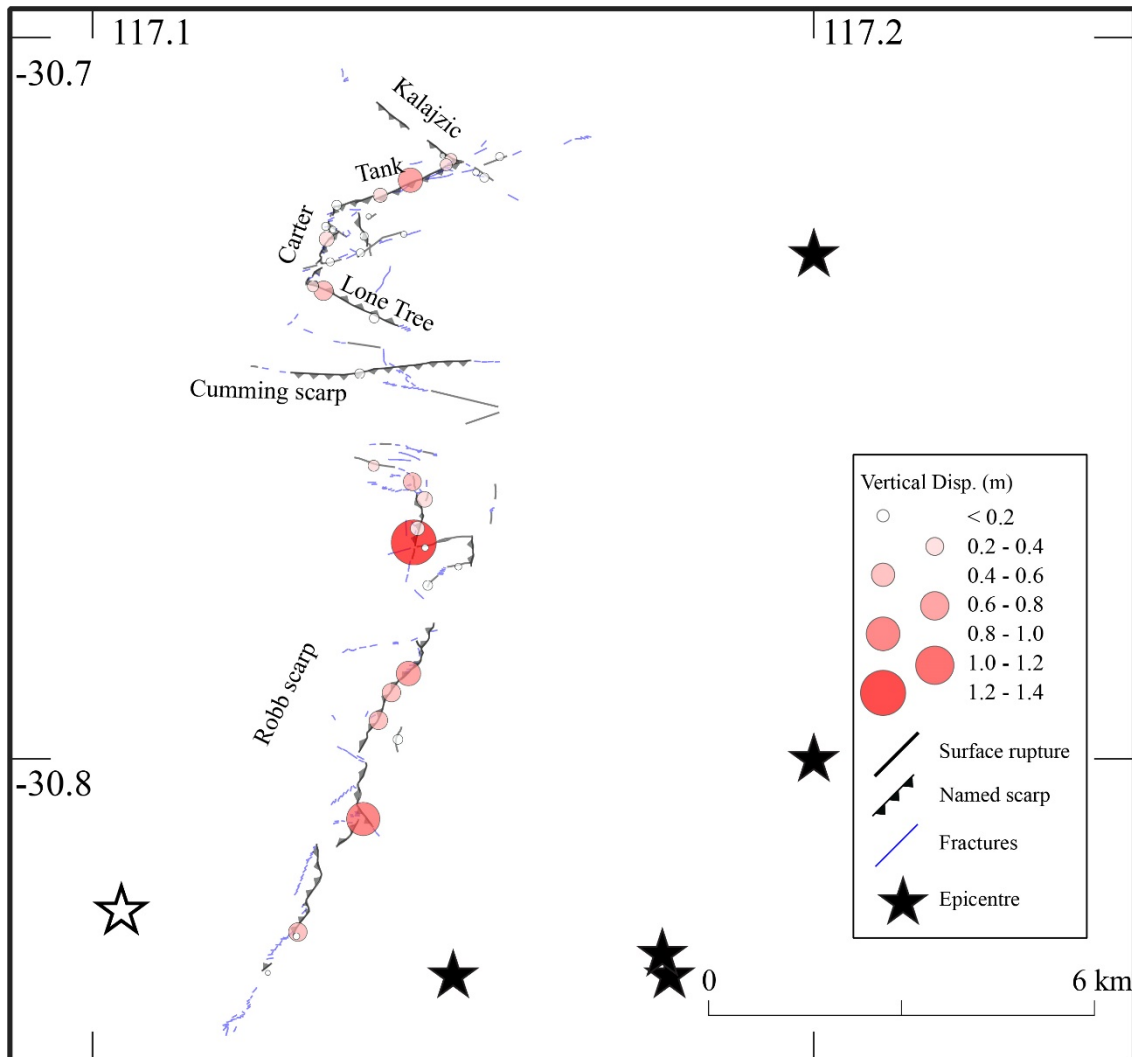


Figure 6: Map of the Cadoux scarps, fractures, vertical offset measurements along the rupture and epicentre locations. Data digitised from Lewis et al. (1981)

3.2 Rupture Morphology

3.2.1. Length and shape

The Cadoux surface ruptures are geometrically complicated. The original map shows nine reverse and strike-slip scarps of different orientations and variable lateral components, connected by a network of fractures and minor ruptures. Lewis et al. (1981) give names to the individual sections including the Robb Fault, Cumming Fault, Lone Tree Fault, Link Fault, Carter Main Thrust, Carter Back Thrust, Tank Fault, Tank Subsidiary Fault and Kalajzic Fault (Figure 6). We refer to features as scarps when describing surface observations which avoids confusion between topographic expression of surface deformation and underlying geological structures (or seismological approximations of geological structures).

Published lengths of the Cadoux rupture are shown in (Figure 7b). These include the sum of all mapped ruptures (28 km Lewis et al. (1981)), and lines connecting all mapped surface features (including fractures 15 km Lewis et al. (1981), only primary ruptures 14 km (Johnston et al., 1994)). Figure 7c

simplifies ruptures to straight lines and defines new faults where mapped primary rupture has gaps/steps > 1 km and/or where strike changes by > 20° for distances > 1 km (e.g. (Quigley et al., 2017)). This results in five faults being defined, explored in more detail in King et al. (2019) (in review). It is unclear whether these faults extend to seismogenic depths.

Figure 7d maps portions of the scarp where more than two vertical displacement measurements of greater than 0.2 m occur within a distance of 1 km (data from Gordon and Lewis (1980)). Given granitic basement cosmogenic erosion rates in equivalent arid settings of Australia of 0.3 – 5 m/Myr (Bierman and Caffee, 2002), 0.2 m of scarp height would be removed within 35 – 660 kyrs, leaving ~12.4 km of rupture still visible in the landscape. This indicates that the feature, while modest, is persistent in the landscape over the time frame typical of the recurrence interval observed on nearby proximal faults (e.g. Hyden, Dumbleyung). In this calculation we do not account for erosion rates of the ferruginous duricrust which may overlie granitic bedrock, for differential erosion rates across the rupture topography, or increased erosion from past climatic changes or modern processes.

The 8 km long Robb scarp is often described as the main thrust portion of the rupture and has a slightly concave shape (relative to its hanging-wall). The network of Lone Tree, Carter and Tank scarps to the north appear to define overall movement along an east-dipping thrust plane. All scarps are discontinuous along their lengths with numerous step-overs and breaks as shown in photos but not necessarily on maps of the ruptures.

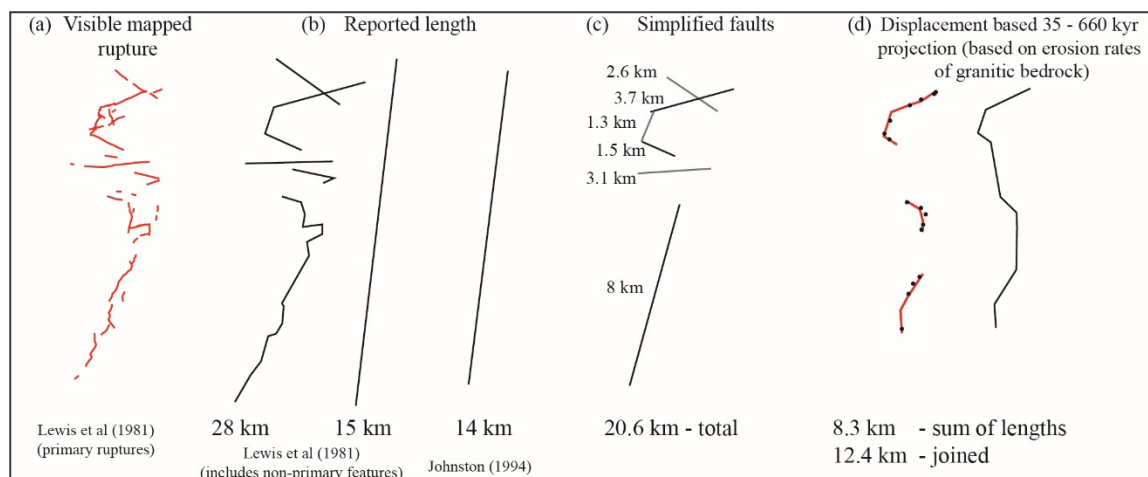


Figure 7: Possible length values across the Cadoux scarps

3.2.2. Strike

The Robb scarp trends towards 201° for the majority of its length. The Lewis et al. (1981) 1:25,000 map shows a sharp change towards 308° along the most northern 2 km of the Robb scarp. The Cumming scarp is 1.3 km north of the Robb scarp and trends towards 087°. The Lone Tree scarp starts 0.6 km north of the Cumming scarp, trends towards 300° and connects into the Carter Main scarp which trends 019° (~80° interior angle). This then connects into the Tank scarp which trends 066° (~130° interior angle) which intersects with the Kalajzic scarp trending 308° (~110° interior angle).

3.2.3. Dip

Lewis et al. (1981) define two predominant fault types based on surface measurements of dip, thrust faults with ~45° dip and high angle reverse faults with 70 - 80° dip. They calculate dips along the Robb Fault based on slip (using lateral, vertical and horizontal displacements) between 42 - 75° (Figure 6) but note that the rupture morphology is more typical of lower-angle thrust fault dips (e.g. 30 - 45°). They consider that the Robb fault may have a steep dip at depth (based on aftershock distributions with poorly defined location and depth), but that dip at the surface may shallow due to lithology. There are no available data to constrain this interpretation.

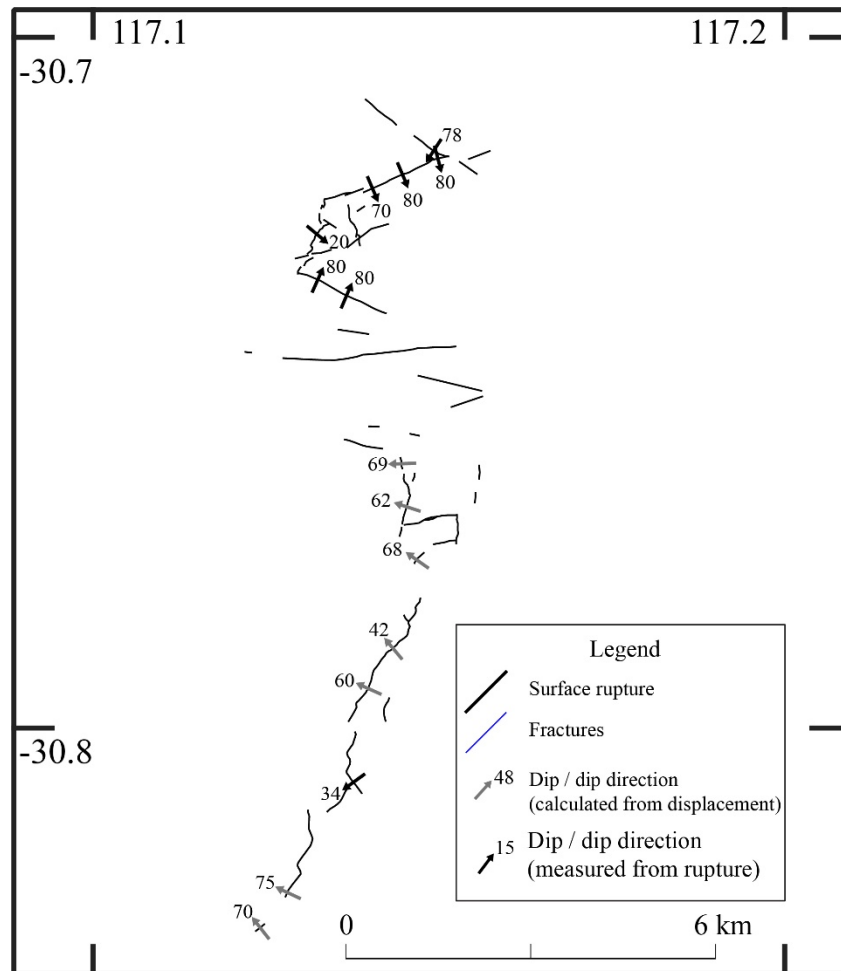


Figure 8: dips calculated or measured for the Cadoux ruptures, digitised data from Lewis et al. (1981)

The Lone Tree scarp has dip measurements of 70° and 85° where the rupture plane is visible (Figure 6). A 1 m deep trench across the Main Carter scarp showed a rupture plane dipping 20° east (Figure 13). The Tank scarp had well exposed rupture planes dipping 70° and 80° south. No dip was visible or calculated for the Cumming scarp. Overall the Lone Tree and Tank scarps delineate steeply dipping faults bounding a shallow east dipping thrust fault (the Main Carter scarp).

3.2.4. Morphology

The central section of the Robb scarp generally forms a single discrete rupture while the northern and southern sections are a complicated series of discontinuous extensional fractures, compressional hummocks, and some short sections of duplexing discrete rupture (in the north only) (Figure 7). The Cumming scarp is described as a linear single discrete rupture for the majority of its length, with little to no “wavy nature” compared to the other scarps (Lewis et al., 1981). The Lone Tree scarp is a relatively straight single discrete rupture (Figure 7), with minor ~ 5 m long duplexing back thrust structures related to compressional sinistral movement (e.g. figure 19, Lewis et al. (1981)). The Carter scarp trace is a discontinuous irregular series of single discrete ruptures, with a back-thrust rupture 400 m to the east in the hanging-wall (the “Carter Back Thrust”) separated by a linear series of *en echelon* fractures (the “Link Fault” in Lewis et al. (1981)). The Tank scarp, similar to the Lone Tree scarp, is described as a simple single discrete rupture, with a number of small splay scarps (i.e. step overs). It is the only known historic Australian event where primary rupture occurs through surface bedrock outcrops (weathered granite), though most have granite in the very near surface (<1 m). The Kalajic scarp is the northern most scarp within the Cadoux rupture complex, and is described as both a simple single discrete rupture, and a series of extensional fractures and hanging-wall warping.

3.3 Kinematics

Predominately dextral movement is recorded from offset fences, roads, farm furrows and en echelon extensional fracture directions along the west dipping Robb scarp (*Figure 10, Figure 11*). No lateral movement was observed along the south-west dipping Cumming scarp. The Lone Tree scarp dips to the north-east with sinistral offsets up to 0.65 m recorded. No lateral displacement is measured along the Carter scarp. The south dipping Tank scarp shows dextral movement where it crosses a rail line and farm furrows, and step-over structures also support dextral compression. The Lone Tree, Carter and Tank scarps are described as a “fault block which moved upwards and westward”, describing a conjugate fault relative to the west dipping Robb scarp. The Lone Tree and Tank scarps accommodate lateral movement (sinistral and dextral respectively) related to hanging-wall uplift towards the west, with the Carter scarp defining the overall direction of compression and main rupture tip. The Kalajzic scarp shows sinistral offset where it crossed pipelines, rail lines, roads and fences

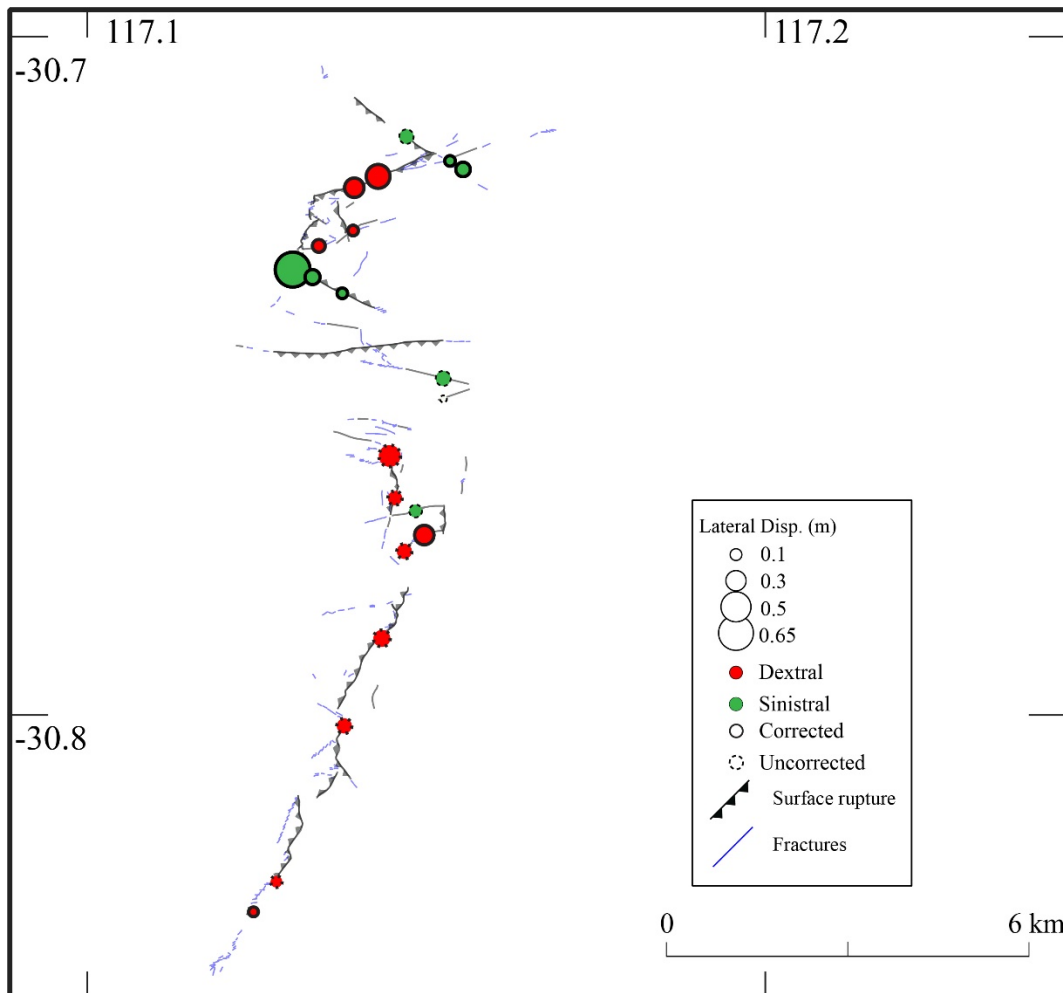


Figure 9: Lateral displacements digitised from Lewis et al. (1981). Uncorrected measurements are offsets measured from features (fences, roads, etc) not perpendicular to the strike of surface rupture.

3.4 Displacement

Cadastral surveys were conducted along offset infrastructure and provided some accurate offset measurements (no uncertainties reported) and profiles across the rupture. However, only the lateral component of movement was measured, which is presented in the profiles of Lewis et al. (1981). Vertical displacement data from offset fences, pipelines, furrows and tree roots is presented on the 1:25,000 map (Lewis et al., 1981). The maximum observed vertical displacement is along the Robb scarp (1.4 m) which shows a median offset of 0.37 m with a west over east sense of movement. The

northern complex of scarps (Carter, Lone Tree, Tank) show median vertical displacement values of 0.2 m with an east over west direction. The Kalajzic scarp at the northern end of the Cadoux rupture shows west over east movement. The only observed vertical displacement values (0.05 - 0.28 m) for this scarp are located close to the intersection with the Tank fault and so may be influenced by the complex interaction of fault geometries. Vertical displacement values were digitised from Plate 2 of Lewis et al. (1981) (see section 6).

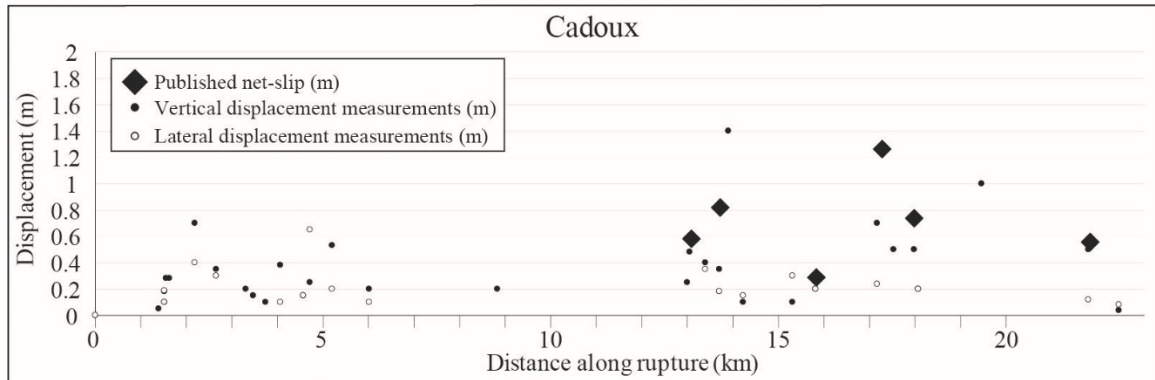


Figure 10: Vertical and lateral displacement measurements along the Cadoux scarps, digitised from (Lewis et al., 1981). Methods described in Appendix A:.

Benchmarks surrounding the Cadoux area were resurveyed following the earthquake along transects 44 km east, 16 km west, and almost 100 km south of the rupture (Lewis et al., 1981) (Figure 11). Based on positive offsets at distances of over 40 km from the Cadoux earthquake, the authors suggest that a $\sim 90 \times 45$ km block east of the rupture has experienced 0.36 m uplift from ‘ground distortion’ associated with the Cadoux earthquake, though they do also note that the uplift may have accumulated aseismically due to tectonic compression. The authors suggest that the measured offset describe an overall east over west sense of reverse movement on the Cadoux rupture. This data may describe coseismic offset along an east dipping fault which reaches the surface along structures with variable geometries (including the 8 km long west dipping Robb scarp). However, the significant distances involved (10 – 40 km) relative to the length over which rupture occurred (14 km), makes the coseismic nature of these offsets questionable. It is considered unlikely that the M_w 6.0 Cadoux earthquake could be responsible for coseismic offset of this extent at the distances involved. The precision and accuracy of the surveys are unknown, but likely to be in the order of a few centimeters.

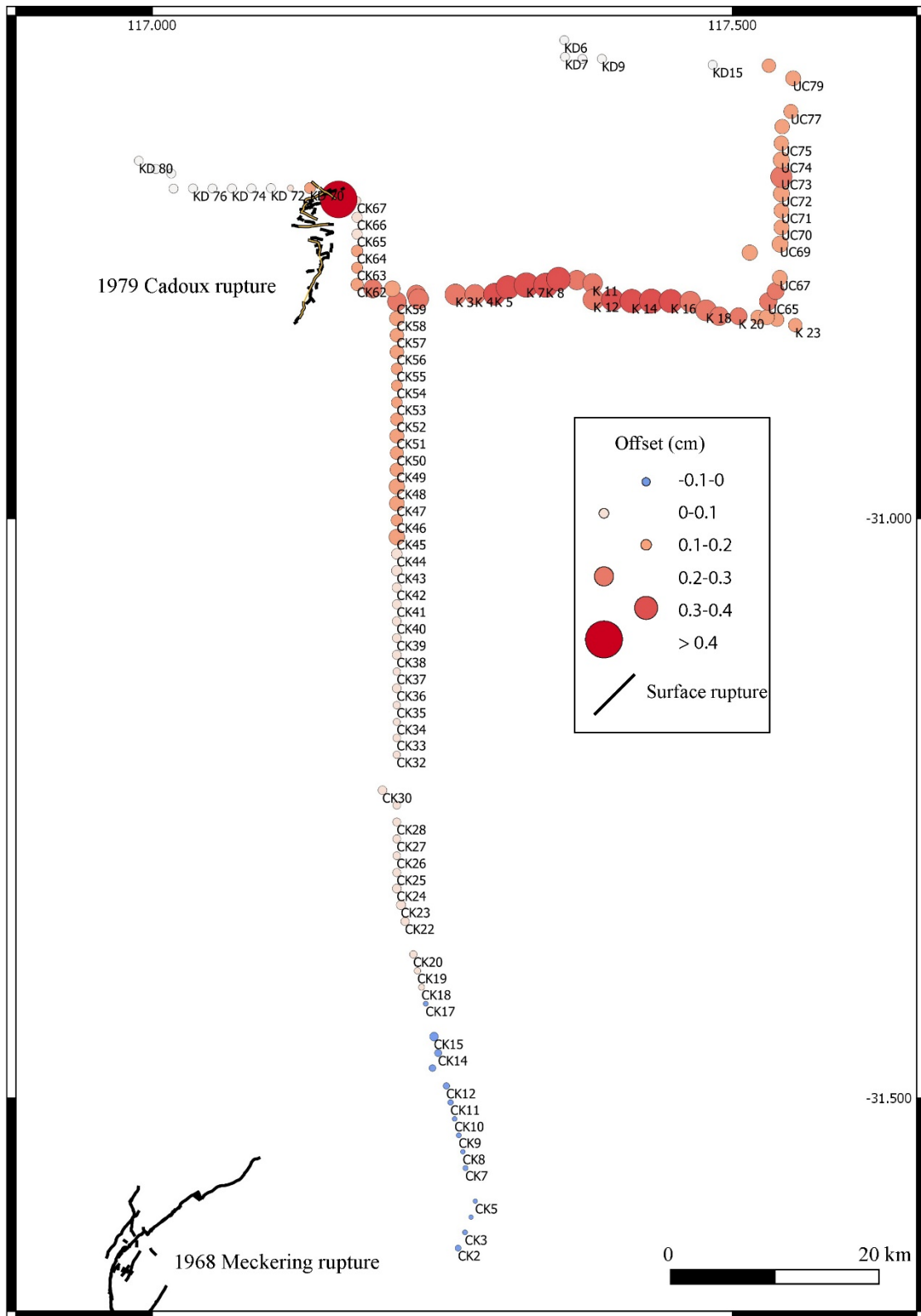


Figure 11. Measurements of offset benchmarks along the “Public Works Department (PWD) water-supply pipeline network”. The original survey was conducted in 1963-1964 and various sections were resurveyed in July 1979, March 1980 and February 1981. (Data digitised from Lewis et al. (1981)). Offsets of up to 0.36 m are seen between Cadoux in the east and Koorda in the west. Uncertainties for these measurements are not described in the publication.

3.5 Environmental damage

Taken together, the length and offset of the Cadoux scarps match an ESI IX, while the length and width of fractures/cracks as described in Lewis et al. (1981) fits ESI V-VI (Michetti et al., 2007). Lewis et al. (1981) investigate bore data from around Western Australia and find that water levels in confined and unconfined aquifers in the Perth Basin and Murchison district show anomalous deviations coinciding with the timing of the Cadoux mainshock. The data for the Murchison district (~500 km north) are less convincing than that of the Perth Basin (~200 km west) (Lewis et al., 1981). If earthquake related, these hydrological events relate to an ESI IV (*“Rare occurrence of small variations in water level in wells and/or the flow-rate of springs”*) (Michetti et al., 2007; Serva et al., 2016). No other environmental damage is specifically documented that falls within the ESI-07 scale. Holes are described along the hanging-wall of the Carter thrust block unrelated to extensional cracking. Similar features are described in King et al. (2018) as related to failure of ‘collapsible soils’ due to seismic shaking (e.g. Rogers (1995)).

3.1 Relationship to Geology

The Tank scarp ruptures through both exposed and thinly covered granite for much of its length. The Kalajzic scarp ruptures within 50 m of weathered and fresh surface outcrops of granite on both the hanging-wall and footwall (the scarp is visible on Google and Bing satellite imagery where fields have not been tilled, -30.71, 117.14 to -30.70, 117.14). The majority of the surface outcrop falls on the hanging-wall of this scarp. The Cadoux scarps roughly align with magnetic anomalies, with a very slight magnetic high on the Robb fault hanging-wall (west side) (*Figure 2*).

Surface bedrock structural fabric measurements align favourably with the northern scarp geometries, but not to the southern Robb Scarp. The steeply dipping Lone Tree and Kalajzic scarps strike in the same approximate direction as bedrock foliations observed to have vertical dips ~8 – 10 km north of the ruptures. The steeply dipping Tank scarp aligns roughly with nearby dykes, with presumed steep intrusion boundaries. The shallow dipping Main Carter scarp strikes in the same direction as nearby outcrop foliations, but these show steeper dips of 50 - 65°. Only one mapped structural measurement shows a westerly dip, ~10 km east of the southern limit of the Robb scarp. East dipping measurements are mapped at a similar distance on the west side of the west dipping Robb scarp.

3.1 Relationship to Seismology

Measurements of surface scarps suggest interacting west, east and south dipping faults and lithological trends along the Cadoux ruptures (Lewis et al., 1981). If the resurveyed benchmarks capture true coseismic distributed deformation related to this earthquake they suggest an overall east over west movement, while the longest section of continuous surface rupture (the 8 km Robb scarp) shows a west over east movement. Lewis et al. (1981) show the mainshock and majority of aftershocks recording up to June 1980 on the east side of the rupture, though these data have high location and depth uncertainties. Relocations of original aftershock data, and data from temporary seismic arrays in the years following the mainshock (1980 – 1983) show zones of high seismicity to the north and south of the ruptures (Denham et al., 1987) and depths supportive of a west dip for the Robb fault (Dent, 1988; Dent and Gregson, 1986). Focal mechanism planes that best match the overall NNE strike of rupture fit steep east dipping (unpublished described in (Lewis et al., 1981)), steep east or west dipping (Fredrich et al., 1988), and steep west dipping solutions (Denham et al., 1987). Boatwright and Choy (1992) analyse P-wave acceleration spectra for the Cadoux earthquake and suggest that broadband time domain records show complex rupture processes.

If each of the Cadoux scarps correspond to through-going faults at depth, the rupture pattern highlights a complex geometry of up to six interacting structures which accommodated coseismic slip. Alternatively, the rupture patterns may support two predominate faults; the west dipping Robb fault and east dipping Carter fault. If the resurveyed benchmarks do show predominate offsets related to

co-seismic east over west movement, and epicentres are correctly located on the east of the ruptures, rupture may have initiated on an east dipping fault at depth and propagated onto shallow bedrock structures resulting in complicated surface scarps. It is not possible to definitively describe the underlying Cadoux fault system without further information (e.g. shallow seismic surveys or reanalysis of original seismic data).

Figure 12 shows a highly simplified cross section based on surface measurements of scarp dips and published epicentre locations and hypocentre depths. The cross section has high uncertainties due to the simplification of complex geometries to a 2D plane, but does show that estimates of hypocentre depths do not match projected fault depths at that location, based on dips derived from surface observations of scarps.

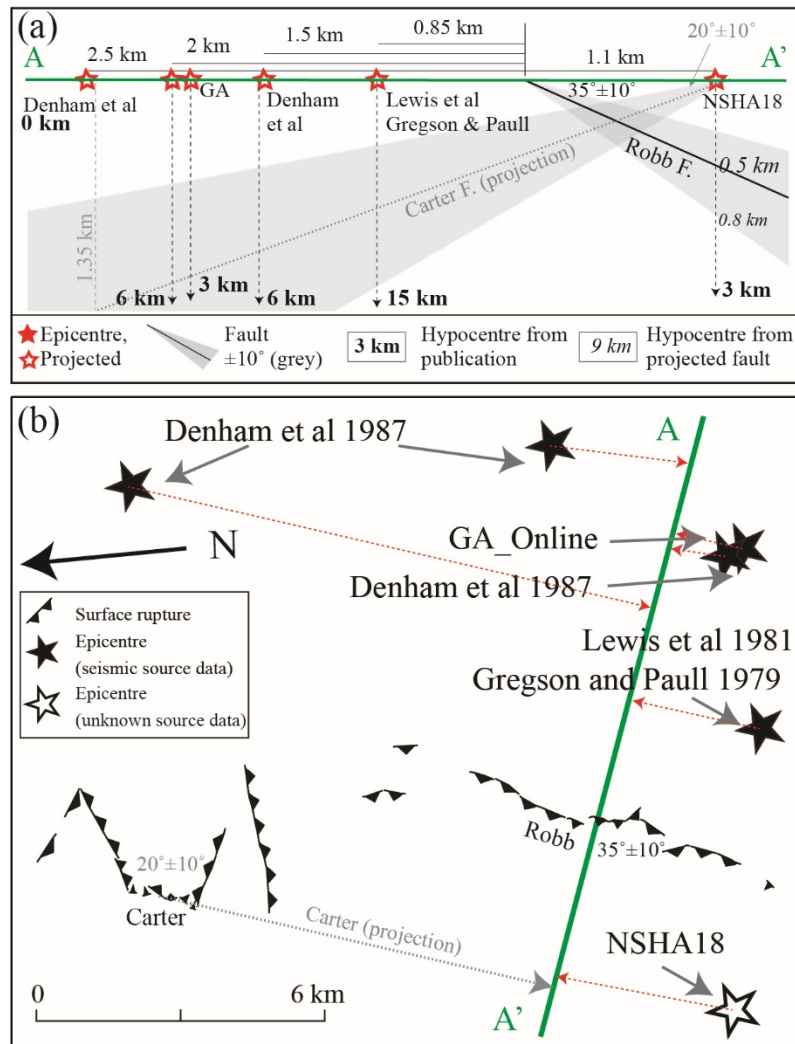


Figure 12: highly simplified cross section of the Robb and Carter scarps as faults using surface measurements of dips ($\pm 10^\circ$), with published epicentres projected onto the cross section showing depth to simplified faults (*italics*), and published depths (**bold**).

The number of distinct faults that are hypothesized to have ruptured in this earthquake ($n=6$), based on the criteria stated herein, is the highest estimate of multi-fault earthquakes at this magnitude as ascertained from a recent global compilation (Figure 13). We hypothesize that this earthquake likely ruptured south-to-north, from an area of relatively simple (Robb fault) to relatively complex crustal structure, that caused a multi-fault rupture cascade.

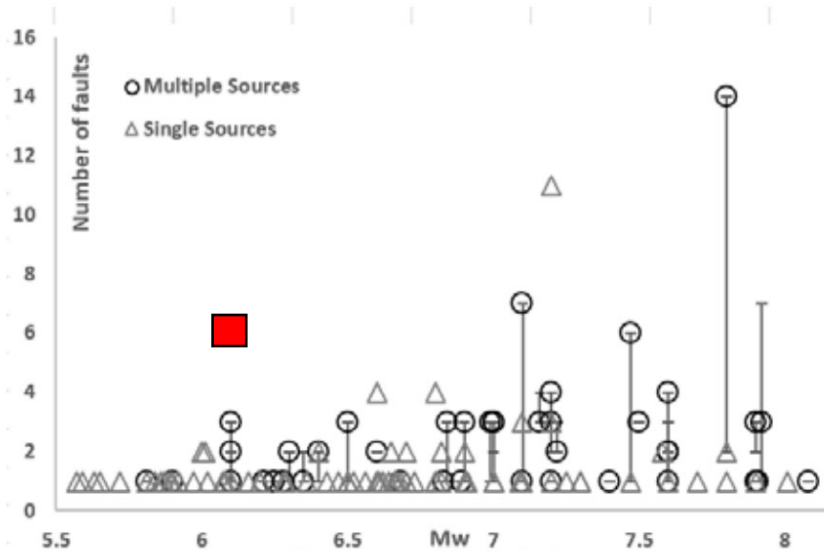


Figure 13: From Fig. 5 of Quigley et al. (2017), Cadoux earthquake (red box) plotted against recent global compilation of number of geometrically-distinguished fault ruptures vs. Mw.

4. Paleoseismology

4.1 Observations pertinent to palaeoseismology of faults

No detailed palaeoseismic investigations of the Cadoux fault have been published. Lewis et al. (1981) describe a 1 m deep trench across the Carter scarp which exposed ~0.5 m of surficial sediments (~0.4 m sand, 0.1 m brown soil) overlying “clayey weathered granite”. These sands are described as Tertiary in age on the available 1:250 000 geological map (Blight et al., 1983). They found offset confined to a single rupture through the granite which split to three ruptures in a narrow band through the sand and to the surface. Bedrock offset in the trench matches offsets at the surface, and the authors describe no pre-existing structures / fault gouge / shear zones in the bedrock, suggesting no relief existed across bedrock prior to 1979.

A second trench is described across the Tank scarp which showed rupture occurred along the edge of a pre-existing quartz vein in the basement granite. The authors interpret this as evidence that at least in this location, faulting was controlled by pre-existing structures. No further information is provided about this trench. Based on the description there is no evidence to suggest the quartz vein was related to prior rupture along this fault. It likely relates to Proterozoic – Archean formation and/or metamorphism and/or deformation of the granite, suggesting no prior rupture in the Cenozoic.

Lewis et al. (1981) note that the Cadoux rupture is roughly coincident with a drainage divide between the North Mortlock River to the west, and salt playas to the east. This topographic divide runs for at least 30 km NNE-SSW.

4.2 Slip rate

Strong evidence exists to suggest that the northern Cadoux scarps (Lone Tree, Carter Main, Tank and Kalajzic) were controlled by basement structures, including the observation of the Tank scarp rupturing along a pre-existing quartz vein within granite and the Kalajzic rupturing coincident with outcrops of granite. This is consistent with previous work across the SWSZ and 1968 Meckering surface rupture (Dentith et al., 2009; Dentith and Featherstone, 2003). No evidence exists to suggest prior Cenozoic rupture on the structures that hosted displacement in the 1979 Cadoux earthquake. The rupture is either the first neotectonic event, or the recurrence interval is sufficiently long that all relief relating to prior event(s) was eroded prior to 1979. If recurrence is assumed, vertical relief generation

rates are limited by very low bedrock erosion rates of < 5 m/Myr (Belton et al., 2004; Bierman and Caffee, 2002).

References

- Allen, T., Leonard, M., Ghasemi, H., Gibson, G., 2018. The 2018 National Seismic Hazard Assessment: Earthquake epicentre catalogue (GA Record 2018/30). Geoscience Australia, Commonwealth of Australia, Canberra, ACT.
<https://doi.org/http://dx.doi.org/10.11636/Record.2018.030>
- Belton, D.X., Brown, R.W., Kohn, B.P., Fink, D., Farley, K.A., 2004. Quantitative resolution of the debate over antiquity of the central Australian landscape: Implications for the tectonic and geomorphic stability of cratonic interiors. *Earth Planet. Sci. Lett.* 219, 21–34.
[https://doi.org/10.1016/S0012-821X\(03\)00705-2](https://doi.org/10.1016/S0012-821X(03)00705-2)
- Bierman, P.R., Caffee, M.W., 2002. Cosmogenic exposure and erosion history of Australian bedrock landforms. *Bull. Geol. Soc. Am.* 114, 787–803. [https://doi.org/10.1130/0016-7606\(2002\)114<0787:CEAEHO>2.0.CO;2](https://doi.org/10.1130/0016-7606(2002)114<0787:CEAEHO>2.0.CO;2)
- Blight, D.F., Chin, R.J., Smith, R.A., Bunting, J.A., Elias, M., 1983. Bencubbin 1:250 000 Geological Map Sheet. Geological Survey of Western Australia, Perth, Australia.
- Boatwright, J., Choy, G.L., 1992. Acceleration source spectra anticipated for large earthquakes in northeastern North America. *Bull. Seismol. Soc. Am.* 82, 660–682.
- Clark, D., 2012. Neotectonic Features Database. Geoscience Australia, Commonwealth of Australia, Canberra, Australia.
- Clark, D., Dentith, M., Wyrwoll, K.-H., Yanchou, L., Dent, V.F., Featherstone, W.E., 2008. The Hyden fault scarp, Western Australia: paleoseismic evidence for repeated Quaternary displacement in an intracratonic setting. *Aust. J. Earth Sci.* 55, 379–395.
<https://doi.org/10.1080/08120090701769498>
- Dawson, J., Cummins, P.R., Tregoning, P., Leonard, M., 2008. Shallow intraplate earthquakes in Western Australia observed by Interferometric Synthetic Aperture Radar. *J. Geophys. Res. Solid Earth* 113, 1–19. <https://doi.org/10.1029/2008JB005807>
- Denham, D., Alexander, L.G., Everingham, I.B., Gregson, P.J., McCaffrey, R., Enever, J.R., 1987. The 1979 Cadoux earthquake and intraplate stress in Western Australia. *Aust. J. Earth Sci.* 34, 507–521. <https://doi.org/10.1080/08120098708729429>
- Dent, V.F., 1988. The distribution of Cadoux aftershocks: Additional results from temporary stations near Cadoux, 1983 (BMR Record 1988/51). Bureau of Mineral Resources, Geology and Geophysics, Canberra, ACT. <https://doi.org/http://pid.geoscience.gov.au/dataset/ga/14238>
- Dent, V.F., Gregson, P.J., 1986. Cadoux microearthquake survey 1983 (BMR Report 1986/022), 1986/22. ed. Bureau of Mineral Resources, Geology and Geophysics, Canberra, ACT.
<https://doi.org/http://pid.geoscience.gov.au/dataset/ga/14114>
- Dentith, M., Clark, D., Featherstone, W.E., 2009. Aeromagnetic mapping of Precambrian geological structures that controlled the 1968 Meckering earthquake (Ms 6.8): Implications for intraplate seismicity in Western Australia. *Tectonophysics* 475, 544–553.
<https://doi.org/10.1016/j.tecto.2009.07.001>
- Dentith, M., Featherstone, W.E., 2003. Controls on intra-plate seismicity in southwestern Australia. *Tectonophysics* 376, 167–184. <https://doi.org/10.1016/j.tecto.2003.10.002>
- Doyle, H.A., 1971. Seismicity and structure in Australia. *Bull. R. Soc. New Zeal.* 9.
- Fredrich, J., McCaffrey, R., Denham, D., 1988. Source parameters of seven large Australian

- earthquakes determined by body waveform inversion. *Geophys. J.* 95, 1–13.
<https://doi.org/https://doi.org/10.1111/j.1365-246X.1988.tb00446.x>
- Gordon, F.R., Lewis, J.D., 1980. The Meckering and Calingiri earthquakes October 1968 and March 1970, Geological Survey of Western Australia Bulletin. Perth.
- Gregson, P.J., Paull, E.P., 1979. Preliminary report on the Cadoux earthquake, Western Australia, 2 June 1979 (BMR Report 1979/215). Bureau of Mineral Resources, Geology and Geophysics, Canberra, ACT. <https://doi.org/http://pid.geoscience.gov.au/dataset/ga/15123>
- Johnston, A.C., Coppersmith, K.J., Cornell, C.A., 1994. The earthquakes of stable continental regions, in: Electric Power Research Institute Report TR-102261-VI. Palo Alto, California.
- King, T.R., Quigley, M.C., Clark, D., 2019. Surface-rupturing historical earthquakes in Australia and their environmental effects: new insights from re-analyses of observational data. *Geosciences*.
- King, T.R., Quigley, M.C., Clark, D., 2018. Earthquake environmental effects produced by the Mw 6.1, 20th May 2016 Petermann earthquake, Australia. *Tectonophysics* 747–748, 357–372.
<https://doi.org/10.1016/j.tecto.2018.10.010>
- Leonard, M., 2008. One hundred years of earthquake recording in Australia. *Bull. Seismol. Soc. Am.* 98, 1458–1470. <https://doi.org/10.1785/0120050193>
- Lewis, J.D., Daetwyler, N.A., Bunting, J.A., Moncrieff, J.S., 1981. The Cadoux Earthquake (GSWA Report 11). Perth, Australia.
- Michetti, A.M., Esposito, E., Guerrieri, L., Porfido, S., Serva, L., Tatevossian, R.E., Vittori, E., Audemard M., F.A., Azuma, T., Clague, J., Comerci, V., Gurpinar, A., McCalpin, J.P., Mohammadioun, B., Morner, N.A., Ota, Y., Roghoshin, E., 2007. Intensity Scale ESI 2007, *Memorie Descrittive della Carta Geologica d'Italia, Special Volume 74*. APAT, Rome 2007.
- Quigley, M.C., Mohammadi, H., Duffy, B.G., 2017. Multi-fault earthquakes with kinematic and geometric rupture complexity : how common ? INQUA Focus Group Earthquake Geology and Seismic Hazards.
- Rogers, C.D.F., 1995. Types and distribution of collapsible soils, in: Derbyshire, E., Dijkstra, T., Smalley, I.J. (Eds.), *Genesis and Properties of Collapsible Soils*. Springer, Loughborough, UK, pp. 1–17.
- Serva, L., Vittori, E., Comerci, V., Esposito, E., Guerrieri, L., Michetti, A.M., Mohammadioun, B., Mohammadioun, G.C., Porfido, S., Tatevossian, R.E., 2016. Earthquake Hazard and the Environmental Seismic Intensity (ESI) Scale. *Pure Appl. Geophys.* 173, 1479–1515.
<https://doi.org/10.1007/s00024-015-1177-8>
- Wilde, S.A., Middleton, M.F., Evans, B.J., 1996. Terrane accretion in the southwestern Yilgarn Craton: evidence from a deep seismic crustal profile. *Precambrian Res.* 78, 179–196.
[https://doi.org/10.1016/0301-9268\(95\)00077-1](https://doi.org/10.1016/0301-9268(95)00077-1)

Appendix A:

Methods for digitising vertical displacement data and benchmark data

Vertical offset measurements for the Cadoux scarp are mapped along the scarp in Plate 2 Lewis et al. (1981). This map was georeferenced against satellite imagery based on the locations of roads, fences, and train tracks. The locations and vertical offset were recorded into a new point shapefile. A simplified fault trace was created for the scarps, and a short script¹ was used in QGIS attribute manager field calculator to extract the distance of each vertical offset measurement along the

¹ `line_locate_point(geometry:=geometry(get_feature('Line', 'id', '1')), point:=$geometry)`

simplified fault trace. The shape file was extracted into a final CSV with x-y coordinates, vertical offset measurements, and distance along fault data.

Vertical differencing from resurveyed offset benchmarks across the Cadoux-Koorda area are presented in Table 12 of Lewis et al. (1981). These show the benchmark name, but no x-y coordinates. The benchmark name and vertical difference data were extracted from a pdf into excel, and thoroughly checked for copy errors in the data. Benchmark locations for the Cadoux region were selected from the Western Australia Geodetic Survey Marks shapefile² and extracted into a CSV file. These benchmark names were cross-referenced against digitise data from Table 12 (Lewis et al., 1981) to assign x-y coordinates of benchmarks to vertical difference measurements.

² <https://catalogue.data.wa.gov.au/dataset/geodetic-survey-marks-point>